Proceedings of the 9th U.S. National and 10th Canadian Conference on Earthquake Engineering
Compte Rendu de la 9ième Conférence Nationale Américaine et
10ième Conférence Canadienne de Génie Parasismique
July 25-29, 2010, Toronto, Ontario, Canada • Paper No 1628

SHAKE TABLE TESTS ON THE COLLAPSE OF REINFORCED CONCRETE FRAMES SUBJECTED TO MODERATE AND HIGH AXIAL LOADS

S. Yavari[1], S-H Lin[2], K.J Elwood[3], C-L Wu[4], S-J Hwang[5], B. Bayhan[6], and J. P. Moehle[7]

ABSTRACT

In order to observe the interaction of structural elements at the onset of collapse, four frame specimens were tested at the National Center for Research on Earthquake Engineering (NCREE) in Taiwan in spring 2009. Each specimen consisted of a 1/2.25 scaled model of a two-bay-two-story reinforced concrete frame. The specimens were tested under moderate and high gravity loads to investigate the influence of axial loads on the collapse vulnerability of the structures. These tests were employed to study the interaction of the beams, columns and joints as collapse was initiated. This paper presents the observations during the tests and comparison of the frame specimen response. An analytical model, simulating the behavior of one of the test frames, is also presented.

Introduction

Many existing reinforced concrete buildings in the United States and worldwide do not satisfy the special seismic detailing requirements of the ACI Building Code (ACI 2008) or similar codes. Employing the provisions from older building codes, most of these structures were designed and constructed with strong beams and weak columns, and lack shear reinforcement in the joint core. Therefore, columns and beam-column joints are more vulnerable than beams to damage or failure in such buildings. Widely spaced and light transverse reinforcement in the columns causes vulnerability to shear failure during ground shaking which results in reduction in building lateral strength, lowering axial load carrying capacity, and potentially leading to collapse of the building.

A major engineering objective is to identify and retrofit such vulnerabilities in existing buildings. To date, there have been relatively few tests on behavior of inadequate reinforced concrete frame systems in the literature, particularly dynamic tests to collapse which limits our understanding of failure and collapse mechanisms. Furthermore, it is observed that in contrast with the frequent collapse predictions based on current assessment procedures (e.g. ASCE 41),

[1]PhD Candidate, Dept. of Civil Engineering, University of British Columbia, Vancouver, Canada,
[2]M.Sc., Dept. of Civil Engineering, National Taiwan University, Taipei, Taiwan
[3]Associate Professor, Dept. of Civil Engineering, University of British Columbia, Vancouver, Canada
[4]Associate Research Fellow, National Center for Research on Earthquake Engineering, Taipei, Taiwan
[5]Professor, Dept. of Civil Engineering, National Taiwan University, Taipei, Taiwan
[6]Visitor Researcher, Dept. of Civil and Environmental Engineering, University of California, Berkeley, USA
[7]Professor, Dept. of Civil and Environmental Engineering, University of California, Berkeley, USA

post-earthquake reconnaissance studies show a relatively low rate of collapse amongst older non-seismically detailed concrete structures even in major earthquakes (Otani, 1999). These observations suggest that current practices for assessing collapse are conservative and need refinement in order to identify the critical buildings that are most collapse-prone.

The following describes a research project that directly addressed this issue through collaboration of researchers from Taiwan, Canada and the United States leveraging knowledge gained in the course of international research programs. The main objective of this work was to experimentally study the seismic collapse behavior of non-seismically detailed reinforced concrete frames. Particularly, this study focused on the investigation of structural framing effects on column shear and axial failures, and conversely, the effects of column failures on frame system collapse vulnerability. Understanding these interactions is essential in assessing the collapse vulnerability of structures. Through a better understanding of mechanisms that cause collapse, improved engineering tools may be developed for use by practicing engineers to assess the collapse vulnerability of poor detailed reinforced concrete frame structures.

Significance of the Research and Project Description

Past shaking table collapse tests have focused on the performance of one specific component (i.e. columns) and only considered low to moderate gravity loads. To fill the gaps in knowledge, this study involved dynamic testing to collapse of four two-dimensional, two-bay-two-story, 1/2.25 scaled reinforced concrete frames at the National Center for Research on Earthquake Engineering (NCREE) in Taiwan. Each frame contained non-seismically detailed columns, commonly referred to as flexure-shear-critical columns, with proportions and reinforcement details that allowed them to yield in flexure prior to shear strength degradation and ultimately reach axial failure. The influence of non-confined joints on the collapse behavior of the frame was also investigated. In particular, the tests focused on two previously unexplored issues: (1) the interaction of multiple vulnerable concrete components (i.e. beams, columns, and joints) within a building frame as collapse is initiated, and (2) the influence of high gravity loads on the collapse vulnerability of a structure.

Fig. 1 describes the types of shaking table specimens that were tested and the names given to each specimen. Comparison of the results from MCFS and HCFS revealed the influence of axial load on shear and axial behavior of flexure-shear-critical columns, while observations from MUF and MUFS demonstrated the effects of unconfined joints on the overall behavior of the frame near the point of collapse and the sequence of failure in the elements. Details of the specimens are described in the following section.

Specimen MCFS:	Specimen HCFS:
Moderate Axial Load	**H**igh Axial Load
Confined Joints	**C**onfined Joints
Flexure-**S**hear Columns	**F**lexure-**S**hear Columns
Specimen MUFS:	**Specimen MUF:**
Moderate Axial Load	**M**oderate Axial Load
Unconfined Joints	**U**nconfined Joints
Flexure-**S**hear Columns	**F**lexure Columns

Figure 1. Description of shaking table specimens.

Specimen Design

The geometries and details for the specimens (Fig. 2) were selected to be representative of elements used in an existing seven-story hospital building in Taichung, Taiwan. Final dimensions and reinforcement details of the frames were influenced by laboratory and shaking table limitations, scaling of column details used in the existing building, available reinforcement, and desired failure mode. The target failure mode was intended to be damage leading to collapse that would enable examination of gravity load redistribution during the test. The ratio of beam stiffness to column stiffness was considered to be similar to the existing hospital building. Since the overall width of the frame, and consequently the beam length, were limited by the dimensions of the shaking table; the beam depth was adjusted to achieve the target beam-to-column stiffness ratio. Beam transverse reinforcement with closed stirrups and 135° hooks provided sufficient shear strength to develop full flexural strength. Beam longitudinal reinforcement was chosen to create a weak-column-strong-beam mechanism typical of the older concrete construction. Neither beams nor columns had lap splices to eliminate the splicing effects from the scope of this study. Slabs were cast with the beams to include the effect of slabs on the beam stiffness and the joint demands.

Beam-column joints in non-seismically detailed concrete frames were frequently constructed without transverse reinforcement and are vulnerable to shear and axial failure during strong ground shaking. However, to separate the collapse behavior due to column failure from that resulting due to joint failure, specimens MCFS and HCFS incorporated well-confined joints and failure of the columns was expected to precipitate collapse of the frame. In contrast, sufficient confinement in the columns of specimen MUF ensured a flexural column response, while eliminating the confinement from the first-story joints was expected to lead to a failure mode dominated by joint shear failure. Constructing MUFS with no confinement in the first-story joints and light transverse reinforcement in the columns provided the opportunity to study the sequence of failure in a typical existing building frame with both unconfined joints and non-ductile columns. Discontinuity of the columns above the second floor made the second-story joints susceptible to early failure; therefore, joints at second level were confined for all specimens.

Given the complexity of desired test frame behavior and failure mechanisms, a detailed analytical model, rather than the common design methods, was used to determine test frame final dimensions and details, considering the common full-scale columns in the existing hospital building. Columns with 200mm × 200mm square section and eight deformed #4 bars for longitudinal reinforcement were selected (longitudinal reinforcement ratio=2.6%). Column transverse reinforcement was selected as 5mm hoops at 120 mm for specimens with flexure-shear-critical columns (MCFS, HCFS, and MUFS), while the spacing was reduced to 40 mm for MUF with ductile columns. The resulting transverse reinforcement ratios for the flexure-shear-critical and flexure-critical columns were 0.16% and 0.49%, respectively. Using ASCE/SEI-41 (2008), the ratio of the plastic shear demand on the columns (V_p) to the nominal shear strength (V_n) varied between 0.9 and 1.0 for the columns in specimens MCFS, HCFS, and MUFS, which complies with the ASCE/SEI-41 definition of flexural-shear-critical columns. V_p/V_n for the columns from the MUF specimen was 0.6, consistent with the ASCE/SEI-41 definition of flexure-critical columns. The average compressive strength of concrete from cylinder tests on test day was 34 MPa, while the yield strengths of the longitudinal and transverse bars in the columns were 412 MPa and 475 MPa, respectively.
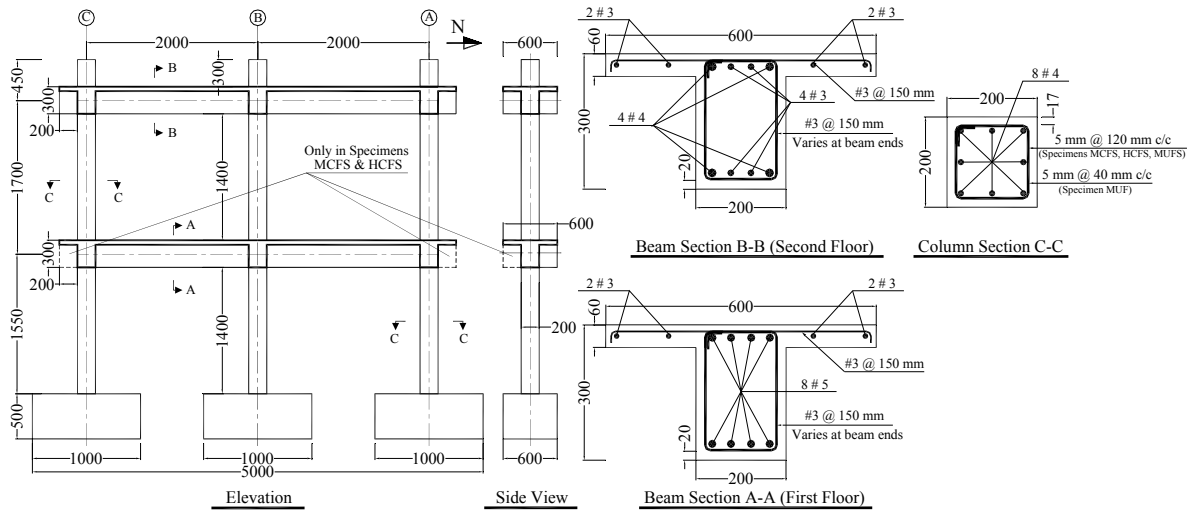
Figure 2. Shaking table test specimen and reinforcement details.

Based on Fig. 2, and for ease of reference throughout this paper, elements of the test frame will be referred to using the following nomenclature. Columns will be referred to by their axis letter and story number; thus, Column A1 is the first-story column at axis A. Joints will follow a similar nomenclature with the number indicating the floor number they are on; thus, Joint A1 is the joint above Column A1.

Loading and Test Setup

Each specimen was constructed vertically, similar to real buildings, in an area outside the NCREE facility and moved onto the shaking table where it was bolted to six load cells (two per column) providing a fixed-base condition for the columns. A stiff steel frame, bolted to the table, was used to brace the specimens in the out-of-plane direction by means of frictionless rollers at each beam level which allow free in-plane motion (both horizontal and vertical) of the frame. Rigid transverse steel beams were connected to the supporting frame to catch the specimen after collapse and prevent any damage to the shaking table.

Additional masses were added to the specimens in the form of lead weights attached to the beams. Loads were distributed equally to all beams, approximately uniformly distributed along beam spans to simulate the loading effects of one-way slabs framing into the beams. The structure was intended to represent a hospital building with higher dead and live load demand than regular residential buildings. Considering the scaling of the frame and loading suggested by the Taiwanese Building Technical Regulations (MOI, 2009) for such occupancy, each beam was loaded with a total weight of 10 kN. Each frame was assumed to be part of a seven-story building and element sizes were selected accordingly; however, only first two stories of the frame were constructed to maximize the scale of the specimen and because damage is normally expected to be concentrated at the base of frame buildings. To account for the inertial forces from the upper stories, inertial-mass with a weight of approximately 100 kN was connected to the frame such that only lateral forces were transmitted to the specimens. The inertial-mass was supported on rollers mounted on the steel supporting frames on either side of the specimen (see Fig. 3). The connection mechanism between the mass and the specimen was designed such that the inertial force could be transferred to the specimen, while the vertical deformation of the columns was not restrained.

The column axial loads from the upper stories were achieved by pre-stressing the columns using pressure-controlled hydraulic jacks allowing for lengthening and shortening of the columns during the shaking table tests. A transverse steel girder, placed on a pin at the top of each column, transferred the axial load to the columns. A clevis pin, aligned with the intended direction of shaking, was installed on each end of the girder. A high-strength threaded rod was used to attach the clevis pin to the hydraulic jack which was secured to the shaking table by another clevis pin. The components of the load in the rods were recorded and the data was adjusted, accordingly. In order to observe the effects of axial load on column and joint behavior, the middle column of Specimens MCFS, MUFS, and MUF was subjected to a moderate axial load of approximately $0.2f'_cA_g=0.16P_0=0.6P_b$, where P_0 is the concentric axial load capacity and P_b is the balanced axial load. The middle column of Specimen HCFS was pre-stressed to an axial load of approximately $0.4f'_cA_g=0.33P_0=1.15P_b$. Note $0.35P_0$ is used by Chapter 21 of ACI-318 to distinguish gravity columns requiring seismic detailing similar to columns of the lateral force resisting system (ACI-318, 2008). The exterior columns of all frames were subjected to half of the axial loads applied to their corresponding middle columns. It should be noted that variation in applied axial load was observed during the tests even though accumulators and fast pressure reducing and relieving valves were used to passively control the axial load at the desired level.
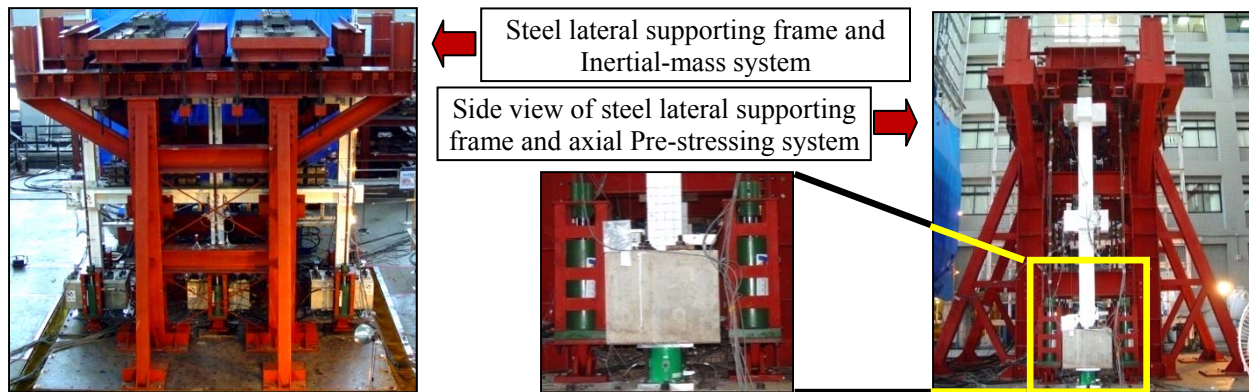

Figure 3. Pre-stressing and inertial-mass system.

All test frames were subjected to the same table motion but scaled to various peak ground accelerations. The north-south component of the ground motion record from the 1999 Chi-Chi earthquake at station TCU047 with the Joyner/Boore distance to the fault of 32.1 km was selected for the tests (recorded PGA=0.4g). This record was scaled to achieve a target PGA of 0.3g (Half-yield Test), 1.1g (Test1), and 1.35g (Test2). Variations in table control resulted in slight variations in the recorded table motions. Table 1 shows the spectral acceleration for the table motion at the approximate natural period for all specimens (0.29 sec), while Fig 4 compares the response spectra for the four specimens during Test2 for the period range up to 1.0 second. Relatively good agreement of spectral accelerations for the different specimens allowed for comparisons the results from the four frames.

Table 1. Test protocol and spectral accelerations.

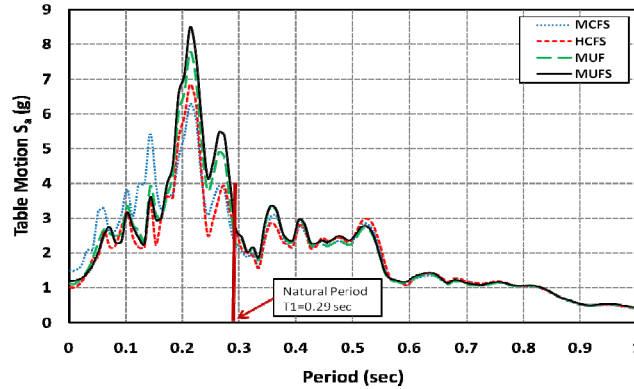| Test Description	MCFS $S_a(T_1=0.29sec)$	HCFS $S_a(T_1=0.29sec)$	MUF $S_a(T_1=0.29sec)$	MUFS $S_a(T_1=0.29sec)$
Half-Yield	0.6g	0.4g	0.6g	0.7g
Test1	1.8g	2.1g	1.8g	1.9g
Test2	2.2g	2.7g	2.2g	2.7g

Figure 4. Elastic response spectra with 2% damping (Test2).

Experimental Test Results

Results from 0.1g White-Noise tests prior to earthquake excitations were employed to attain the natural period and damping ratio of the frames. The natural periods of the specimens were obtained in a range of 0.28 to 0.29sec, while the damping ratio was determined to be 3%. All the frames sustained very minor flexural cracks (less than 0.1 mm), during the Half-Yield Test. The specimens did not collapse during Test1, but all of them were to some extent damaged. As expected, columns of frames MCFS and HCFS experienced shear and flexural cracks, while damage was mostly concentrated at the exterior first-story joints of specimens MUF and MUFS. Results from another White-Noise test after Test1 revealed that the natural period of the specimens was increased, where specimens MCFS and HCFS experienced a period of 0.36 sec and specimens MUF and MUFS experienced a longer period of 0.46sec. The specimens did not perform similarly during Test2 and the failure mode was different for each frame (Figure 5). Specimen MUF did not collapse during Test2, while the other three frames experienced complete collapse. Frame MCFS collapsed due to shear and axial failure of the first-story columns. This was not observed for the other cases, where combination of plastic hinge development and damage to the structural elements caused the failure of the frame.
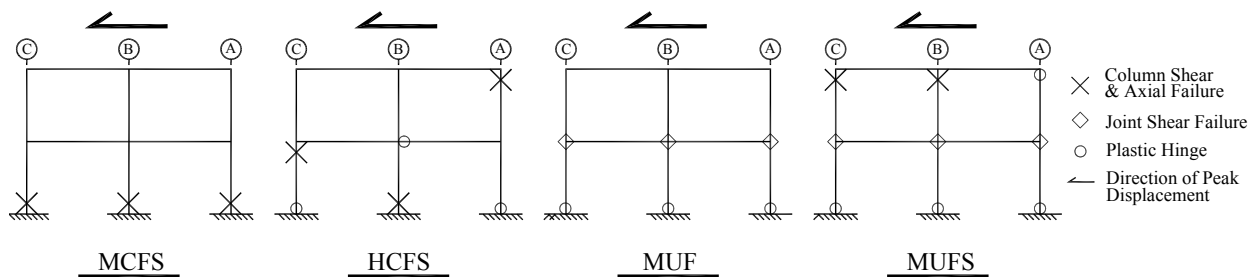

Figure 5. Failure mode for each test frame.

During Test1, frames experienced story drifts large enough to cause yielding and shear cracks in specimens MCFS and HCFS (2.2% drift ratio), and joint shear cracks in specimens MUF and MUFS (2.8% drift ratio). Largest frame drift during Test2 was experienced by frame MCFS (6.7%), where all of the first-floor columns failed. Unlike specimens MCFS and HCFS, the maximum drift ratio of specimens MUF and MUFS, with unconfined joints, remained similar during both Test1 and Test2. This can be explained by the localized shear deformation at the joints, where large shear cracks developed in joint area decreasing the frame stiffness.

Nevertheless, the joints did not cause the collapse of the specimens. Fig. 6 compares the base shear hysteretic response of the four frames for Test1. It is observed that the columns in specimens MUF and MUFS did not reach their plastic shear capacity, while their first-story drift ratio was larger than MCFS and HCFS. Flexural yielding of columns may be expected for specimen MUF with ductile columns, however, similar performance by specimen MUFS, with flexure-shear-critical columns, suggests that the unconfined joint in these two specimens worked as a fuse and did not allow shear to be fully transferred to the first-story columns and accommodated much of the deformation demands. This is supported by the hysteretic response from Test2 (Fig. 7), where unlike MUF and MUFS, the first-floor columns from MCFS and HCFS failed under the lateral demand.
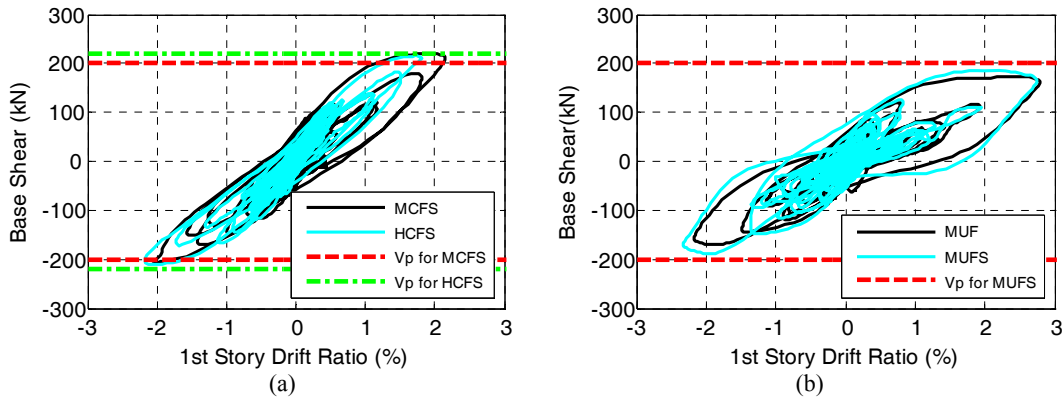

Figure 6. Comparison of base shear hysteretic response of the frames during Test1 (a) MCFS vs. HCFS; (b) MUF vs. MUFS.
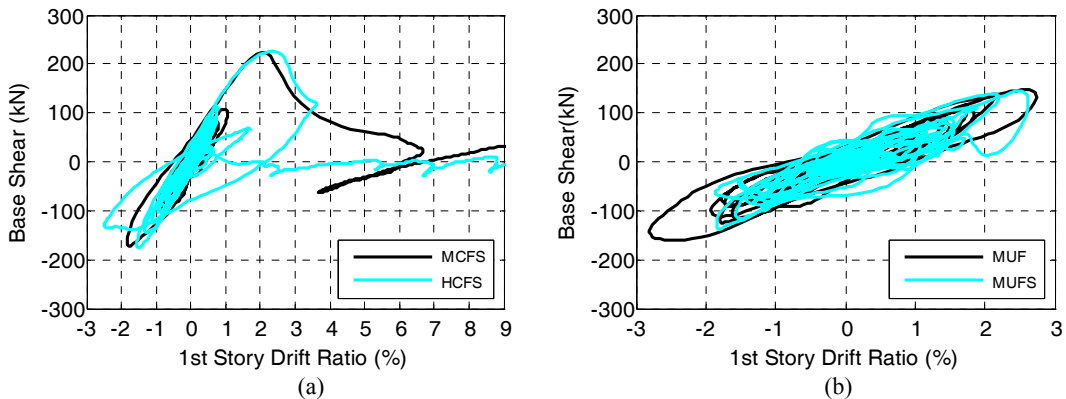

Figure 7. Comparison of base shear hysteretic response of the frames during Test2 (a) MCFS vs. HCFS; (b) MUF vs. MUFS.

For the sake of brevity, only the behavior of columns in specimens MCFS and HCFS are compared here. Due to negligible elongation of the connecting beams, columns A1, B1, and C1 underwent almost equal story drifts. However, the initiation of shear failure was at a different time and drift ratio for each column because of different axial loading. As discussed earlier, columns experienced shear failure only during Test2. In specimen MCFS, shear failure of column B1 was initiated at approximately 1.9% drift ratio and the peak shear of 79.5 kN. Column C1, taking higher shear forces due to overturning compression demands, experienced shear failure at 2.2% drift ratio and shear of 87.2 kN. Finally, column A1 at a drift ratio of 2.8% and shear of 65.7 kN commenced to fail. Shear failure initiation can be defined where shear

strength loss starts and large shear cracks are developed. Shear hysteretic response of first-story columns of specimens MCFS and HCFS are compared in Fig. 8. It is observed that the onset of shear failure happened at a slightly larger drift ratio for specimen HCFS, where column B1 experienced shear failure at 2.3% drift ratio and a shear of 86.8 kN and shear failure of column C1 was commenced at 2.9% drift ratio and a shear of 81.6 kN. However, column C1 did not lose all its shear capacity in the same cycle as B1. Unlike frame MCFS, column A1 of specimen HCFS did not experience significant shear degradation. It was noticed that after shear degradation in columns B1 and C1, column A1 experienced additional tension and the first-story beam between columns A1 and B1 experienced flexural yielding resulting in shear failure of column A2. More observations from the shaking table tests and comparison of the test results can be found in the study by Yavari (Yavari, 2010).
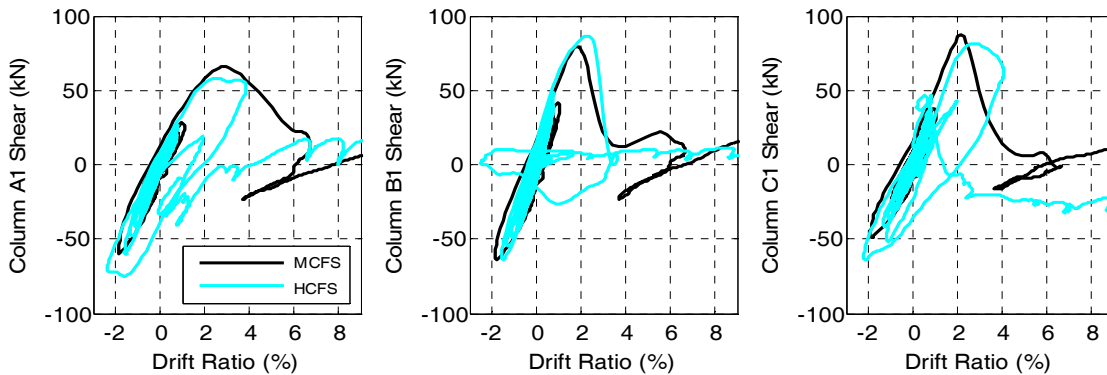

Figure 8. Comparison of shear hysteretic response of first-story columns of specimens MCFS and HCFS during Test2.

Comparison of Test Data with Analytical Model

This section compares the experimental test results for specimen MCFS with an analytical model developed using OpenSEES, a finite-element analysis platform designed for earthquake engineering simulation (OpenSEES, 2009). Fig. 9 shows a schematic of the model for the specimen. Each column consisted of a single nonlinear beam-column element with 5 integration points and two zero-length elements located at the top and bottom of the beam-column element. Each of the zero-length elements was defined by two nodes at the same location. The nodes were connected by multiple material objects to represent the force-deformation relationship for the element. The top zero-length elements for the columns included shear and axial springs with behavior that were defined by LimitState material models used to capture shear and axial failure of concrete columns (Elwood, 2004). To account for the flexibility due to slip of the longitudinal reinforcing bars, elastic rotational slip springs, with rotational stiffness recommended by Elwood and Eberhard (2009), were included in zero-length elements at both ends of column elements. The beams did not exhibit a significant degree of nonlinearity during testing; therefore, for computational efficiency, they were modeled as elastic with lumped plasticity rotation springs at the face of the joints to account for flexibility due to bar slip. The equivalent flexural stiffness for the beam was derived from moment-curvature analysis, which produced a flexural stiffness parameter, $EI_{flex} = 0.4EI_{gross}$, where E is the concrete modulus of elasticity and I_{gross} is the gross section moment of inertia. Joints in specimens MCFS and HCFS were well-confined by transverse beams and reinforcement and therefore, the results presented here were obtained using a rigid joint model.
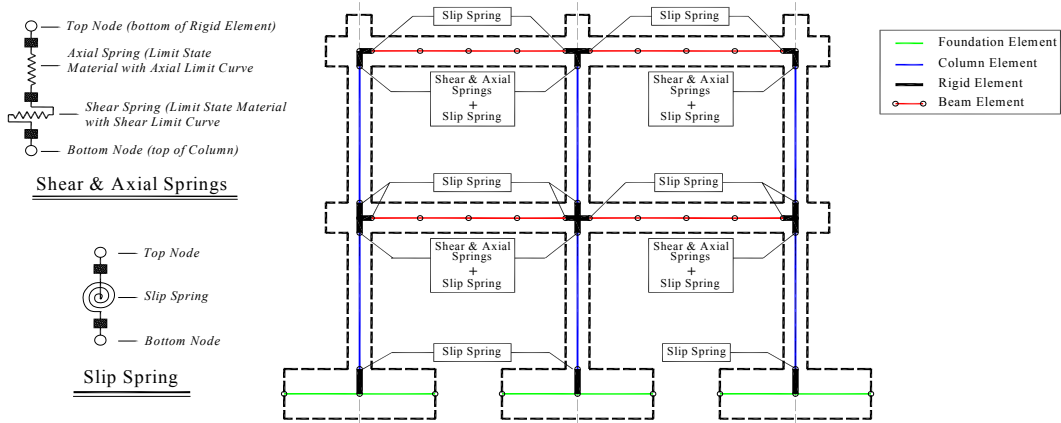
Figure 9. Model of shaking table specimen MCFS.

Similar to the observations from the experimental tests, the analysis demonstrated concentrated damage in first-story columns, with relatively less damage in upper-story columns prior to collapse. Results of analysis for shear and axial behavior of column B1 of specimen MCFS are shown in Fig. 10. Due to detailing and material properties of the columns, drifts at shear and axial failure of each column were very close, and therefore, the analysis became very sensitive to the drift capacities determined in the model for the shear and axial springs. Employing the original model for drift capacities (Elwood, 2004), the analytical model predicted the shear and axial failures in Test1, while shifting the drift capacities by only 0.1% leaded to accurate prediction of the failure in Test2 and not Test1. However, this refinement also resulted in shifting the predicted drift capacity for column B1 during Test2. At drifts of 2.3% and 2.4%, shear failure was detected for columns B1 and C1, respectively. Between 2.3% and 3.0% horizontal drift, a rapid loss of shear resistance was observed in columns B1 and C1. Axial failure of column B1 was initiated at 2.8% drift, followed by axial failure of column C1 at 3.0% drift. Analysis was terminated after failure of column C1 due to instability of the frame resulting in a lack of convergence in the analysis.
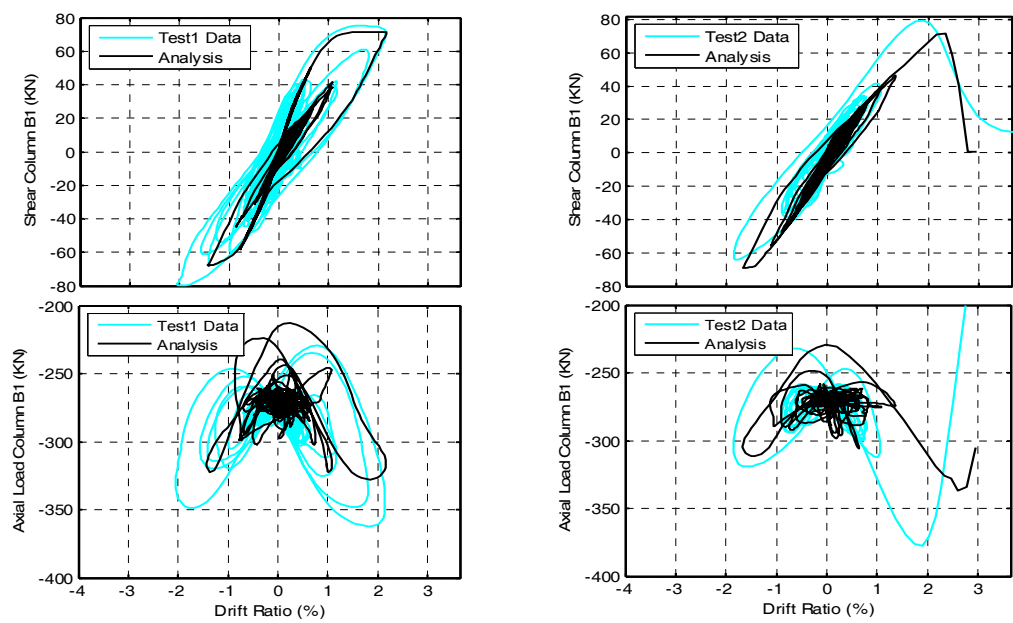

Figure 10. Shear and axial behavior of Column B1 of Specimen MCFS during Test1 and Test2.

It was observed that the predicted behavior of columns using the analytical model was generally in agreement with the results from the experimental test. While the maximum drift of the frame was accurately captured during Test1, the analytical model underestimated the strength of the frame. This can be explained by the influence of strain rate on the strength of the elements. A very high velocity of 1.05 m/s was recorded during Test1, where the strength of the columns considerably increased due to the increase in material strength at this high loading rate. Nevertheless, such effect was not considered in the dynamic analysis. Further research is required to provide recommendations on how to incorporate strain rate effects in nonlinear dynamic analysis.

Summary and Conclusions

Four frames with non-seismic details were tested in the National Center for Research on Earthquake Engineering under moderate and high axial loads. Details of the specimens and setup of the tests were described in this paper. Observation of interaction of failure in columns and joints during the tests suggests that frame detailing and layout of critical elements are crucial in determining failure sequence and ultimately collapse mechanisms. Furthermore, comparison of results from testing specimens under moderate and high axial load indicates that changes in axial loads can significantly impact the failure mode for the frames.

Due to material properties and detailing, drifts at shear and axial failure of the non-ductile columns in the test frames were very close. Modeling of such building frames is very sensitive to estimation of drifts at shear and axial failure. Moreover, the results suggest that to achieve high fidelity in the analysis results, the influence of strain rate on the strength of elements should be taken into account for shaking table tests.

Acknowledgment

References

American Concrete Institute (ACI), 2008. Building *Code Requirements for Structural Concrete, ACI 318-08*, Farmington Hills, USA.

American Society of Civil Engineers (ASCE), 2008. Seismic Rehabilitation of Existing Buildings, *ASCE/SEI 41 Supplement 1*; American Society of Civil Engineers, Reston, USA.

Elwood, K.J., 2004. Modeling Failures in Existing Reinforced Concrete Columns, *Canadian Journal of Civil Engineering* 31 (5), 846-859.

Elwood, K.J. and M.O. Eberhard, 2009. Effective Stiffness of Reinforced Concrete Columns, *ACI Structural Journal,* 106 (4), 476-484.

OpenSEES, 2009. Open System for Earthquake Engineering Simulation. Pacific Earthquake Engineering Research Center, University of California. http://www.opensees.berkeley.edu.

Otani, S., 1999. RC Building Damage Statistics and SDF Response with Design Seismic Forces. *Earthquake Spectra* 15 (3), 485-501.

Ministry of the Interior (MOI), 2009. Building Technical Regulations, *Construction and Planning Agency, Ministry of the Interior,* Taipei, Taiwan, ROC, (in Chinese).

Yavari, S. 2010. Experimental and Analytical Studies on Dynamic Behavior of Multi-Story Reinforced Concrete Frames with Non-Seismic Detailing, *PhD Dissertation, Department of Civil Engineering, University of British Columbia,* Under Preparation.